HUMAN EMOTION SYSTEMS LABORATORY PREPRINTS

Mapping the Human Emotion Circuits with Positron Emission Tomography

Lauri Nummenmaa[1,2] & Jussi Hirvonen[1,2]

[1]Turku PET Centre and Department of Psychology, University of Turku, Finland
[2]Turku University Hospital, University of Turku
[3]Department of Radiology, Turku University Hospital, University of Turku

Address correspondence to
Lauri Nummenmaa
Turku PET Centre c/o Turku University
Kiinamyllynkatu 4-6, 20520 Turku, Finland
Fax +358 2 231 8191
Email: latanu@utu.fi

Abstract

Positron emission tomography (PET) is the most sensitive technique for imaging of human physiology and molecular pathways *in vivo*. Here we provide an overview of PET instrumentation and modelling and illustrate how different PET techniques can be used for mapping the molecular basis of human emotion circuit. We first cover the principles of PET imaging and the most common imaging targets, modelling methods, and experimental designs in brain-PET. We then describe how metabolic studies and neuroreceptor mapping of the endogenous dopamine, opioid, serotonin, and cannabinoid systems have contributed to our understanding of the emotional brain. Finally, we review the recent state-of-the art developments in PET-fMRI, total-body PET and discuss how these techniques can transform the landscape of systems-level biological imaging of the emotion circuits across the brain and periphery.

Outstanding questions

- How different neuroreceptor systems interact when generating distinct emotional states?
- What kind of brain-periphery networks coordinate different emotions?
- What is the relationship between glucose utilization, cerebral perfusion, and haemodynamic responses during acute emotions?
- How epigenetic regulation in the human brain contributes to the pathogenesis of neuropsychiatric disorders?

1. Molecular imaging of the emotion circuits *in vivo*

Positron emission tomography PET is the most sensitive technique for imaging physiology and molecular pathways in living humans. Compared with imaging modalities with high spatial (e.g., magnetic resonance imaging, MRI) and temporal (e.g., magnetoencephalography, MEG) resolution, PET provides unique insight into human brain anatomy and physiology through its unparalleled chemical resolution. The capability to image specific molecules in living human tissue provides unique opportunities from drug development to basic scientific research on higher mental functions. PET relies on complex instrumentation, particularly when short-lived radioisotopes are used, as this necessitates on-site radiochemistry laboratories with cyclotrons for isotope production. Although long-lived isotopes are available commercially for clinical use, these are not always suitable for the type of questions asked in affective neuroscience. Accordingly, PET has remained an underrepresented tool in the affective neuroscience community, particularly compared to cheaper methods with easier instrumentation, such as functional MRI. Despite this complexity, PET is a critical tool in affective neuroscience due to its unique radiochemical and contrast generation mechanism and resultant high chemical resolution. Here we provide an overview of PET instrumentation and modeling and illustrate how different PET approaches can be used for mapping the molecular basis of human emotion circuits.

1.1. Principles of PET

PET allows in vivo molecular-level imaging of biological processes using positron-emitting radiotracers. Radiotracers are molecules with specific biological properties (vehicles) that are chemically combined or radiolabeled with positron-emitting radionuclides. The biological interaction between the molecular vehicle and the targeted tissue provides the basis for studying biological processes. The radiochemical properties of the unstable radionuclide allow the quantification of PET signal, which is generated by the annihilation of an emitted positron with an electron in the tissue (*1*). The most common radionuclides (Table 1) are [^{18}F] (fluorine-eighteen), [^{11}C] (carbon-eleven), and [^{15}O] (oxygen-fifteen), but numerous others are also used. The unstable isotope decays through β^+ decay resulting in a nuclide with one proton less and one neutron more, and a positron (e^+) and a neutrino (ν) are emitted. When the positron travels through tissue ($\sim$ 1mm) it loses kinetic energy, ultimately colliding with an electron (e^-). This results in an annihilation event where two 511 keV photons are emitted in opposite directions.

PET imaging is based on the simultaneous detection of these photons in a small temporal window by scintillation detectors arranged in a circular shape around the gantry (**Figure 1**). The line between a pair of scintillators is called the line of response (LOR), and the scanner continuously records the confidence events for all possible LORs. Thus, the PET camera measures changes in regional radioactivity over time. The image is reconstructed based on the localization of the annihilation events for each detected coincidence. In older PET cameras, the annihilation event is calculated on the LOR based on the attenuation of the positron while it travels through the tissue. Although numerous photons are emitted *almost* simultaneously, modern PET cameras can also implement time-of-flight information (*2*): Picosecond-rate measurements of the time difference between detecting the photons released during coincident events allow even more accurate determination of the annihilation site.

The spatial resolution of PET scans is technically limited by the size of the photon detectors, but also by the random positron scatter before the annihilation events. The theoretically maximal resolution for clinical studies is estimated to be slightly below ~3mm full width at half maximum (*3*). The temporal resolution varies depending on the kinetics of the radiotracer. Common fluorine-based isotopes in clinical use, such as [^{18}F]FDG, have a temporal resolution of tens of minutes to hours, whereas short-lived radiotracers with H_2[^{15}O] may allow sub-second temporal resolution with the ultra-sensitive total-body PET cameras (*4*). Chemical sensitivity for PET is approximately

10^{-12} – 10^{-9} mol, and chemical resolution (specificity) is usually ~K_i 100x lower than for closest resembling molecules. High sensitivity is the property of the PET scanner instrumentation, mostly due to its ability to detect even minuscule amounts of radioactivity. This allows the measurement of targets even with low density in the tissue. In contrast, high specificity (chemical sensitivity) is the property of the radioligand and the target protein because the PET scanner only measures radioactivity over time, regardless of its origin. Therefore, it cannot separate specific (target) and non-specific (off-target) binding. Radiochemical and preclinical testing of the radioligand is needed to ensure that the radioactivity signal mostly represents specific binding to the intended protein target. To put the above-mentioned performance characteristic numbers into context, the spatial resolution is slightly lower than routine T2* EPI sequences used in functional imaging and significantly lower than modern T1-weighted structural MR sequences but substantially better than in MEG. Temporal resolution is well beyond real neuronal timescale and what can be achieved with T2* EPI, but for fastest tracers, it approaches the timing of slow-acting neuromodulatory effects (tens of seconds). Sensitivity greatly surpasses that of MRI.

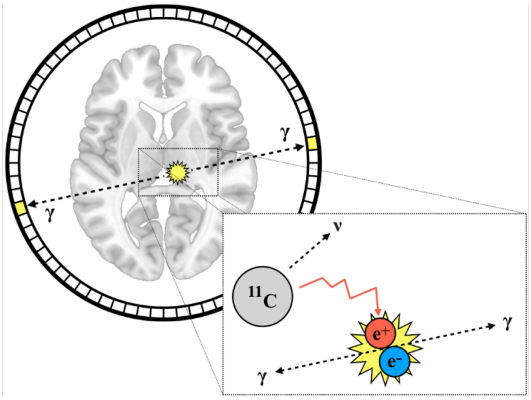

Figure 1. Principle of PET imaging. *In β^+ decay a positron and a neutrino are emitted. Positron travelling through the tissue loses energy and is annihilated upon colliding with an electron. Two 511 keV photons are emitted in opposite directions and picked up by the detectors on the line of response. Image courtesy of Dr Tatu Kantonen.*

1.2. Modelling the PET data

The PET signal generated by the photon coincidences indexes simply raw radioactivity at a given place and time. The goal of pharmacokinetic modelling is to use time-activity information for estimating physiological parameters such as perfusion, metabolic rate, or receptor density. Radiotracer accumulation is influenced by multiple factors ranging from radiotracer metabolism and urine extraction. These can be accounted for in the kinetic modelling, where physical parameters are estimated based on the raw radioactivity and thus transformed into biologically meaningful information. For example, activity from glucose metabolism tracers such as [^{18}F]FDG can be modelled to yield estimates of glucose metabolism per second, H_2[15]O activity can be modelled to estimate blood flow and so forth. The modelling varies greatly across radiotracers and imaging protocols, but the following five main approaches (ordered from least to most accurate) can be considered:

1. **Analyzing raw radioactivity counts.** This allows visualization of the image, but the data are not comparable across subjects and tissues because the number of counts varies depending on the injected activity and subjects' mass, because fixed activity will be distributed more widely in larger subjects. Furthermore, this kind of unstandardized rank order measure is not biologically informative.
2. **Standardized uptake value (SUV) modelling.** This approach accounts for uptake differences by controlling image-derived radioactivity concentration for injection and

subject weight and can thus be considered as a semi-quantitative method. It makes comparisons between subjects (from calibrated scanners) possible with minimal modelling, yet it does not represent data in specific physiological or biological units (*5*). Both raw radioactivity count and SUV measurements only consider total radioactivity, regardless of the signal source (specific or non-specific).

3. **Tissue ratio methods.** By calculating the ratio of tissue radioactivity concentrations over time, the uptake of a region of interest can be related to that in a reference region. This is a crude estimate of specific binding and, unlike full kinetic modeling, does not consider the time course of radioactivity concentrations.
4. **Simplified reference tissue modelling.** If ex vivo studies have established that the radiotracer has high binding in target of interest and minimal binding in some other region, these low-binding regions can be used as a reference for quantifying tracer uptake, as all the tracer in the reference region can be considered as unspecific due to lacking tracer targets. Consequently, regional uptake can be quantified as the ratio between specific regional uptake and the unspecific uptake in the reference tissue (*6, 7*).
5. **Full kinetic modelling.** If absolute quantification of PET images is desired, dynamic (i.e., 4D) scan and input function describing the non-metabolized radiotracer needs to be acquired, ideally from arterial plasma or blood, and potentially the analysis of radiotracer metabolites from blood. When combined with knowledge of the biological mechanisms of the tracer interaction with the tissue, this approach allows the most accurate biological modelling.

Radiotracer	Stable molecule	Isotope	Half-life	Target
[18F]FDG	Fluorine [F]	[18F]	118 min	Glucose metabolism
[11C]flumazenil	Carbon []	[11C]	20 min	GABA receptors
[13N]ammonia	Nitrogen [N]	[13N]	10 min	Perfusion
[15O]H2O	Oxygen [O]	[O15]	2 min	Perfusion
[11C]raclopride	Carbon [C]	[11C]	20 min	Dopamine D2 receptors
[18F]fallypride	Fluorine [F]	[18F]	118 min	Dopamine D2 / D3 receptors
[11C]diprenorphine	Carbon [C]	[11C]	20 min	μ, δ, and ϰ opioid receptors
[11C]carfentanil	Carbon [C]	[11C]	20 min	μ-opioid receptors
[carbonyl-11C]WAY-100635	Carbon [C]	[11C]	20 min	Serotonin 5HT1A receptors
[11C]MADAM	Carbon [C]	[11C]	20 min	Serotonin 5HTT transporters
[18F]FMPEP-d_2	Fluorine [F]	[18F]	118 min	CB1 endocannabinoid receptors

Table 1 Properties of some common PET radiotracers.

1.3. Imaging targets for brain-PET

Whereas in MRI the image contrast is generated by the pulse sequence, in PET the contrast is dependent on the interaction of the vehicle and the tissue. Thus, radiochemistry is the limiting factor in developing new imaging targets. Radiotracer development is, however, difficult as a desirable tracer must fulfill numerous criteria: it has to be safe, have high uptake in the target tissue, can pass the brain-blood barrier (in the case of brain imaging), metabolites not interfering with kinetic modelling, and fast enough kinetics to allow quantification in a reasonable time. When considering the imaging of the emotion circuits, the brain provides many challenges as a target tissue from the radiochemical perspective. To cross the blood-brain barrier (BBB), the radioligand must be sufficiently lipophilic (fat-soluble), but not excessively lipophilic to avoid high non-specific

binding to off-targets in the tissue (such as vessel walls and cell membranes). In addition, the radioligand should not be a substrate to any of the efflux transporters at the BBB (such as P-glycoprotein, P-gp). Radioactive metabolites should not cross the BBB because the PET camera cannot separate between specific and non-specific binding. Some fluorine-18 radioligands are defluorinated, and the resultant 18-fluoride may be taken up by the skull, which may interfere with measurements from the adjacent cerebral cortex. Finally, the radiochemistry must be simple enough to allow reliable routine production. Due to these limitations, all relevant targets cannot be imaged with PET, and for example, usable tracers for imaging the human oxytocin system remain to be developed (*8*). PET imaging targets relevant to affective neuroscience can be divided into two broad categories: i) perfusion, ii) metabolism, and ii) neurotransmission and neuromodulation-related targets, including receptors, transmitters, and transporters (**Figure 2**). Due to kinetics of different radiotracers, the studies can be run using different experimental designs (**Box 1**). In the next sections, we outline how imaging these three broad target categories can be studied in the context of affective neuroscience.

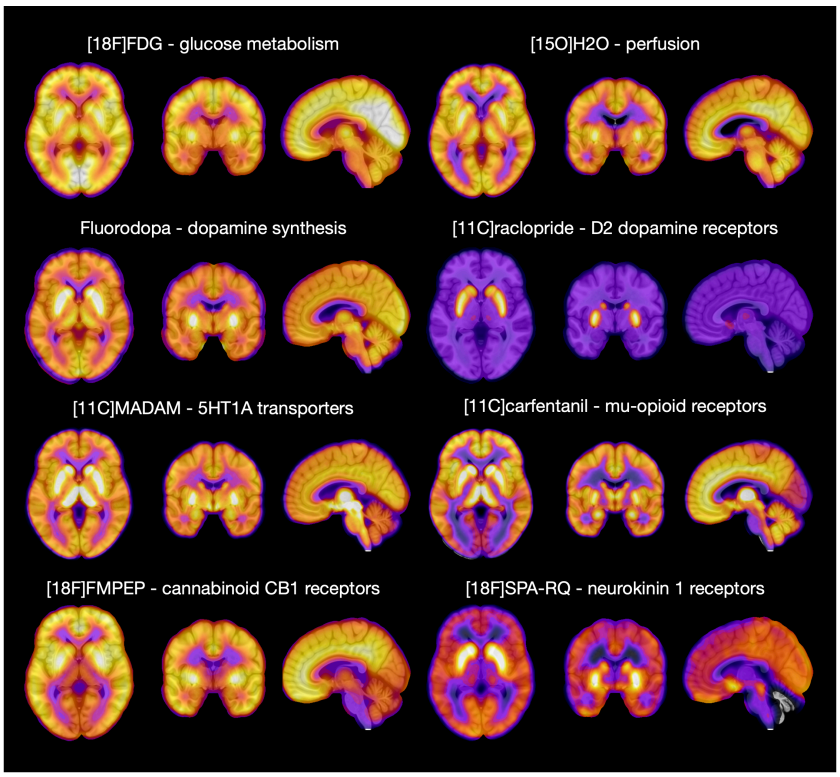

Figure 2: *Illustration of the uptake of radiotracers commonly used in PET studies on the emotion circuits. Data courtesy of Turku PET Centre.*

Box 1. Most common designs used in PET studies in affective neuroscience

1. **Cross-sectional design**, where outcomes of a single scan are compared between groups or correlated against biological or psychological variables in a single group. Examples involve comparisons of neuroreceptor availabilities in different patient groups (*9*) or the links between receptor availabilities and (*10*) personality characteristics.
2. **Longitudinal design** where radiotracer uptake is measured repeatedly under neutral baseline conditions. This design can be used with all radiotracers as long as tracer decay is allowed between the scans. For example, one PET study using this kind of design showed how baseline availability of mu-opioid receptor systems is lowered in obese subjects, but recovered following weight loss (*11*).

3. **Challenge design** where radiotracer uptake is measured at during neutral baseline and pharmacological, physiological, or psychological challenge. This can be done either on two separate scans or during single scan withs separable baseline and challenge parts. This design is possible with all radiotracers if they are sensitive to the experimental manipulation and radiotracer decay is allowed between the scans. A classic example is receptor occupancy studies, where the capacity for the drug (e.g. selective serotonin reuptake inhibitors) to occupy to its target (serotonin transporter 5-HTT) is measured using a radioligand ([^{11}C]DASB) that competes against same binding sites (*12*). This design can also be used with nonpharmacological challenges such as pain (*13*), where the stimulus-evoked release of the endogenous ligand (opioid peptides) competes with the binding sites of the radiotracer ([^{11}C]carfentanil), thus contrasting measurements during rest and stimulation allow estimating endogenous ligand release based on the competition.
4. **Activation design** where brain activation is measured repeatedly during different task conditions such as emotional stimulation (*14*) using a boxcar-shaped stimulation model. To obtain meaningful temporal resolution and to allow separation of task-related activity across blocks, radiotracer must be allowed to decay between blocks. Thus, this approach is practically limited to measurements of cerebral perfusion with short-lived H2[^{15}O] and measuring activation of, for example, neuroreceptor systems with the current carbon and fluorine labeled receptor radioligands necessitates the slower challenge design.

2. Quantified perfusion and metabolic imaging

Functional imaging of the human brain with radiolabeled water H_2[15]O (radiowater) became possible in the 1980s. Because water is biologically inert, radiowater passes through the body in the vessels, and measuring the resulting gamma can thus be sued for quantitative perfusion measurements. It is commonly used in mapping, for example, myocardial blood flow, for detecting ischemia (*15*). Because radiowater has a short half-life, it also allowed the first volumetric brain activation studies where repeated H_2[15]O boluses are given during different task blocks. This approach was pivotal for *in vivo* mapping of human mental functions ranging from emotions (*16*) to cognition, yet it is limited by the accumulating radiation load from the repeated radiowater injections: because H_2[15]O is a short-lived (half-life 124 s) radiotracer, signal decays quickly after injection and repeated injections are needed. Yet due to subject safety, the number of boluses has to remain sufficiently low, hampering signal-to-noise ration. The resultant temporal resolution is also in the rank of tens of seconds at best. Since the advent of functional magnetic resonance imaging (*17*) and particularly the even-related designs leading to efficient experimental protocols (*18*), truly quantitative perfusion-based PET studies of human brain activity fell out of favour due to the complexity, low temporal precision, and associated radiation burden. However, radiowater PET was a pioneering approach in functional tomographic imaging, and the early studies mapping the human emotion circuits paved the way for the widely used statistical parametric mapping approaches for localizing brain functions, including emotion networks (*16*). Despite advancements in perfusion measurements with, e.g., arterial spin labeling using MRI, the PET-based perfusion measurements provide quantifiable biological measurements of cerebral physiology.

Cerebral glucose metabolic rate (GMR) indicates the allocation of the brain's energy resources. In PET, glucose uptake can be measured using glucose analog radiotracer [18F]-FDG. In steady-state conditions, FDG is taken up into cells in competition with other sugars, phosphorylated by hexokinase, and trapped inside the cell. This phosphorylation results in a polar entity that cannot diffuse from the cell. Because cerebral glucose utilization is tightly associated with neural spiking frequency (*19*), baseline glucose metabolism can be used to measure tonic baseline activation of the brain during rest. These intrinsic brain functions are related to predicting and responding to different environmental challenges similar to in "resting state" fMRI (*20*). The radioisotope's long

half-life (109.7 minutes) essentially precludes conventional activation studies like those with radiowater (but see section 4.1). Nevertheless, slower phasic changes in cerebral metabolism, such as those occurring during anesthesia (*21*), can be readily quantified with FDG-PET. An important advantage of FDG imaging is that it can capture brain metabolism retrospectively: If the radiotracer is injected prior to the experimental manipulation, trapping of FDG during the task varies as a function of regional metabolic demands, and due to the long half-life of FDG, the signal can still be measured tens of minutes after tracer delivery. For example, this approach has been used in primates to quantify brain networks involved in the natural communicative signalling so that the FDG was injected before the monkeys were allowed to communicate, and PET scan was performed afterwards (*22*). Because elicitation of natural emotional reactions such as extreme fear, sexual arousal, or aggression is difficult to accomplish inside PET or MRI bore, this technique could allow mapping metabolic brain basis of highly natural emotional responses, yet these kinds of studies are yet to be conducted.

Performing FDG-based activation studies is technically possible yet complicated (see **section 4.1** below), but in turn, FDG is well suited for cross-sectional studies across groups with affective pathologies because the FDG signal can be accurately quantified. Altered metabolism in the insula, limbic system, basal ganglia, thalamus, and cerebellum have been consistently linked with major depressive disorder (MDD) in volumetric meta-analyses of PET data (*23*). Relatedly, large-scale cohort studies have found that allostatic load with subclinical depression (and stress) is linked with regional glucose uptake changes in otherwise healthy individuals (*24*). Several FDG-PET studies have also established that perturbations in the emotion regulation system such as pathological aggression are associated with lowered prefrontal and increased subcortical brain function in murderers (*25*). Finally, the amygdala is known to be a central structure involved in fear and anxiety (*26*) and tonic differences in baseline regional glucose metabolism in the primate central nucleus of amygdala are associated with anxious phenotype as measured by standardized behavioural testing (*27*). Because brain-wide association studies require substantial sample sizes (*28*) and due to the invasive nature of PET imaging, dedicated studies targeting the links between psychological and behavioural variables are rare. However, standardized behavioural and clinical testing in the conjunction of calibrated PET scans with [18F]FDG across projects can lead to the accumulation of a large cross-sectional database, where links between brain glucose utilization and affective and metabolic variables can be addressed (*24, 27, 29*).

3. Neuroreceptor systems

Synaptic neurotransmission allows communication between neurons, and having more than one neurotransmitter system leads to substantial plasticity in the functioning of the central nervous systems, for example, by allowing different spatial scales and inhibitory and exhibitory systems. *In vivo* neuroreceptor imaging (**Figure 3**) is a unique feature of PET, as no other imaging technique allows investigation of the receptor systems in the living human brain with similar accuracy. The timescale of the fastest-acting GABAergic and glutamate systems is beyond the temporal resolution of PET, but radiotracers targeting the GABA-A receptors, such as [^{11}C] and [^{18}F] labeled flumazenil can be used to index tonic receptor levels. Particularly the GABAergic system is relevant for affective imaging, given that benzodiazepine-type drugs bind to GABA-A receptor subtypes, leading to the anxiolytic, addictive and motor effects (*30*). Unfortunately, they are not sensitive to GABAergic activity changes (*31*). Several radiotracers have been tested for glutamate receptors, but their usability for in vivo human studies has remained limited (*32*). In the context of affective neuroimaging, the systems most widely studied with PET are the endogenous opioid, dopamine, serotonin, and endocannabinoid systems. These neuroreceptor systems are broadly linked with mood, motivation, and several desirable PET radiotracers exist for each system. We will next review how PET imaging of these systems has helped in understanding of the emotional brain.

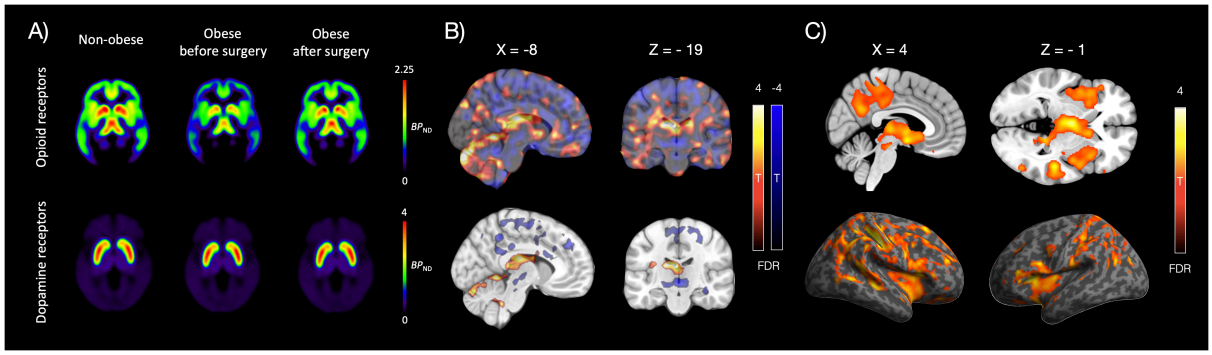

Figure 3. *Neuroreceptor imaging of the opioid system with PET. A) Longitudinal data shows how endogenous mu-opioid receptor (but type 2 dopamine receptor) system is downregulated in morbid obesity, but recovers following bariatric surgery induced weight loss. B) Nonpharmacological challenge study shows how availability of MORs is lower following social laughter versus neutral baseline condition, indicating endogenous opioid peptide release. C) Cross-sectional correlational study showing how endogenous opioid receptor availability is negatively associated with subclinical depressive symptoms. Adapted from (11, 33, 34)*

3.1. Dopamine system

The dopamine system is a key modulator of goal-directed behavior, emotion, cognition, and motor functions. Multiple PET radiotracers exist for imaging the dopamine system (**Table 1**). Of these, the [^{11}C]raclopride (*35*) has probably been most widely used due to its desirable pharmacokinetic properties and easy modeling, selective D2R binding, and sensitivity to endogenous dopamine levels, permitting "challenge" studies of endogenous dopamine release. The early neuropsychiatric studies, motivated by the D2R blocking mechanism of antipsychotic drugs, established altered baseline D2R binding and (*36-39*) increased amphetamine-induced dopamine release in schizophrenia and other psychotic disorders. Thereafter, aberrant dopaminergic neurotransmission has consistently been observed in numerous addictive disorders (*40*). Alcohol and drug dependence are linked with lowered D2R availability (*41-43*), while results are less consistent in behavioural addictions and addiction-like behaviours. For example, pathological gambling is not associated with altered D2R availability (*44*). Animal have found striatal D2R downregulation in obesity (*45*), while human studies have yielded mixed results with some finding lower (*46-48*) and others unaltered (*49-51*) D2R availability in the striatum. Thus, substance abuse likely downregulates the D2R system via direct pharmacological effects, whereas behavioural addictions and addiction-like states are modulated via different pathways. PET studies using the radioligand [11C]raclopride in humans have also consistently demonstrated DA release in central pathways during reward processing. Dopamine is release following meal consumption (*52*) but not following intravenous glucose challenge (*50, 51*), suggesting that that the dopamine signal relates to hedonic responses driven by the orosensory and chemical taste pathways. Studies have also demonstrated rewards such as listening to one's favorite music (*53*), gambling (*44*) playing video games (*54*), or even rewards associated with simple task switches (*55*) lead to striatal dopamine release. However, negative emotions also induce DA release in the amygdala, lateral frontal cortex and striatum during processing of negative emotional words (*56, 57*), thus it is possible that the effects pertain general-level engagement of the motivational or motor systems.

3.2. Opioid system

Among the three classes of opioid receptors (μ, δ, and ϰ), the μ receptors mediate the effects of endogenous β-endorphins, endomorphins, enkephalins, and various exogenous opioid agonists (*58*). The predominant action of μ-opioids in the central nervous system is inhibitory, but they can also exert excitatory effects, and MORs are expressed widely throughout the human emotion circuits (*59, 60*). Multiple PET radiotracers are available for quantifying OR, with [11C]diprenorphine (binding to μ, δ, and ϰ receptors) and [11C]carfentanil (binding to μ,

receptors) being the most widely used (**Table 1**). Both are suitable for conducting challenge studies, allowing functional mapping of opioid system activity. While dopamine system downregulation is consistently observed in drug addictions, the results on the opioid system are less clear-cut. Alcohol dependence is associated with increased MOR availability in striatal sites (*61, 62*), and cocaine dependence similarly results in similar yet more widespread effects (*63*). Conversely, chronic abuse of opiates is associated with down- rather than upregulation of MORs (*64, 65*), suggesting drug-specific effects in addictive disorders. Downregulated μ-receptor action has however been established as one of the key pathophysiological mechanisms underlying obesity (*9, 11, 66-68*). Yet, as MOR dysfunctions are not observed in behavioural addictions such as pathological gambling (*69*), these effects might reflect metabolic rather than reward-related consequences of weight gain.

Clinical, pharmacological, and behavioural studies have consistently linked the MOR system with both antinociception and hedonia and PET studies using the challenge paradigm have consistently shown that both pain and pleasure elicit endogenous opioid release. The initial studies established that nociceptive stimuli reliably trigger opioid release in striatum and thalamus (*13, 70, 71*), but comparable effects are also observed for various primary rewards such as feeding (*68, 72*), sex (*73*), social contact (*33*), and physical exercise (*74, 75*). Opioid release has also been found following "abstract" secondary pleasures, such as internally generated pleasures following mental imagery. These effects extend beyond primary rewards, for example, positive moods induced by mere mental imagery (*76*). These seemingly opposite results on MOR activation during pain and pleasure likely reflect the general role of the MOR system in regulating arousal during stressful events and also during relaxation during the positive mood. Indeed, a recent large-scale study found that the downregulation of MORs is consistently associated with subclinical levels of depression and anxiety. It is thus possible that pathophysiology in this stress buffer system could lead to clinically significant depressive symptomology, but so far, the clinical PET studies on ORs in major depression have yielded mixed results (*77, 78*).

3.3. Serotonin and endocannabinoid systems

The serotonin system is consistently implicated in mood regulation. Altered serotonergic neurotransmission is one of the most important molecular markers of depression (*79*) and the most widely used antidepressants increase extracellular serotonin levels by inhibiting the serotonin transporter (SERT). Multiple PET tracers have been developed for imaging the 5HT1A receptors (e.g., [^{11}C]WAY) and SERT (e.g., [^{11}C]MADAM). PET meta-analyses have found that serotonin transporter availability is systematically lowered in patients with depression (*80*). This is supported by genetic studies suggesting that variability in serotonin transporter mediates how stressful life events may lead to depression (*81*). The most studied serotonin receptor, the 5-HT1A receptor, is expressed as a presynaptic autoreceptor in the raphe nuclei, where the cell bodies of the serotonergic neurons are located, and as postsynaptic receptors at target brain regions, mostly cortical brain areas. In major depression, PET studies have shown both increased (*82*) and decreased (*83*) binding in patients with major depression compared with healthy controls. These inconclusive results may be due to clinical heterogeneity and differences in radioligand quantification methods (*84*). Disturbances of the 5-HT1A receptor have also been demonstrated in other mood disorders, such as bipolar depression (*85*). More recently, novel radioligands have allowed the demonstration of alterations in mood disorders in other serotonergic targets, such as the 5-HT4 receptor (*86*), 5-HT1B receptor (*87*), and amphetamine-induced endogenous serotonin release (*88*).

CB1 receptor (CB1R) is the most abundant G-protein coupled receptor in the mammalian brain, mediating the effects of endogenous (such as anandamide and 2-AG) and exogenous (such as tetrahydrocannabinol) cannabinoids (*89*). CB1R modulates various affective functions, such as

reward and stress. For example, injecting CB1 agonists to the shell of nucleus accumbens increases food intake (*90*) and comparable hedonic responses. CB1R can be studied with various radioligands, including [^{11}C]MePPEP (*91*), [^{18}F]FMPEP-d_2 (*92*), [^{11}C]OMAR (*93*), and [^{18}F]MK-9470 (*94*). Studies in addictive disorders with [^{18}F]FMPEP-d_2 have shown spatially and temporally specific patterns of CB1R abnormalities (*95*). In chronic cannabis users, CB1R availability is downregulated in cortical areas, but it recovers after abstinence, suggesting that neuroplasticity in the CB1R system might underlie cannabis addiction in the brain (*96*). This downregulation has been confirmed with other radioligands [REF]. In patients with chronic alcoholism, CB1Rs are downregulated throughout the brain, and this downregulation is not reversed after abstinence (*97*). Tobacco smokers also show a slight downregulation of CB1R (*98*). Human PET studies have also found decreased CB1R availability in males with a high risk for obesity, indicating that aberrant CB1R function might predispose to overeating and obesity (*9*). This is further corroborated by cross-sectional correlational data indicating that CB1R availability is negatively associated with a broad range of negative feeding-related traits, such as emotional and restrained eating (*99*). In sum, PET studies have confirmed the role of CB1R in reward processing, addictive disorders, and food intake and obesity, but the specific role of CB1R in the human emotion circuits remains to be fully elaborated.

4. Beyond the current state of the art: PET-MRI, total-body PET, and novel targets

Despite its long history, PET is still an actively evolving technology. In addition to developments in radiotracer libraries, hardware components, and modelling and analysis methods, the PET community has recently witnessed two major changes in the way we acquire PET data: The introduction of simultaneous PET-MRI devices, and more recently, the advent of total-body PET for simultaneous mapping of the whole-body biological circuits. In the final sections we discuss how these techniques are transforming the PET field in the context of affective science. We also discuss some new molecular imaging targets in the brain.

4.1.PET-MRI

Multimodal or fusion imaging allows combining information across different imaging targets for studying interactions of biological systems. Although technically data from all tomographic modalities can be combined if the images can be coregistered, in affective neuroscience, the most significant developments have been made with combined PET-MR imaging. The simplest possible approach involves separate PET and functional MR imaging sessions and fusing the temporally separated datasets. This sacrifices the temporal mapping between the modalities, but with PET imaging targets with slow tonic changes this approach allows addressing the relationship between, for example, regional metabolism or neuroreceptor levels and task-induced haemodynamic responses. For example, a large bulk of studies have shown how metabolic dysregulation and obesity are associated with aberrant cerebral glucose utilization (*9, 29, 100*), and PET studies have further shown how the basal glucose metabolism drives transient stimulus-dependent responses in the reward circuit, providing link between tonic and phasic reward circuit functions (*101*). This approach is even more powerful when combined with PET imaging of receptor targets and BOLD-fMRI of affective functions. For example, endogenous baseline MOR availability (as measured with PET) is consistently and negatively linked to haemodynamic responses to different psychological stressors (*102, 103*). Similarly, limbic and prefrontal serotonin system tone modulates limbic BOLD-fMRI responses to emotional stimuli (*104-107*), revealing specific neuromoldulatory effects on the regional haemodynamic activity.

More recently, the PET-fMRI imaging has shifted the focus towards truly simultaneous multimodal imaging with MRI scanners equipped with PET detector rings. There are trivial gains from the simultaneous PET-MR imaging such as speeding up the patient workflow as PET and MR images can be acquired simultaneously. The technique also improves coregistration of the MR

and PET data as the patient can remain positioned during both scans. The latter effect is most significant for organs such as the gut that moves around in the abdominal cavity, but it also important for rigid organs such as the brain. Although the BOLD-fMRI has desirable spatial and temporal resolution for functional neuroimaging and the studies are simple to run on any modern MRI device, their major downside is the complex physiology behind the haemodynamic signal (*108*). Accordingly, typical fMRI studies cannot yield truly quantitative indices of e.g., brain metabolism, perfusion, or spiking frequency, but instead they provide a net index of blood oxygenation and perfusion (*109*). Furthermore, the BOLD-fMRI is unspecific with respect to the underlying neurotransmission. Simultaneous fMRI combined with biologically specific PET imaging can thus aid in understanding the physiological basis of the BOLD signal.

Recently, novel experimental techniques have been developed for measuring dynamic changes in task-induced glucose utilization changes using slow boxcar designs during [18F]-FDG infusion (*110*). In this approach, slow-frequency stimulation model (task on vs. task off) is set up akin to blocked fMRI designs, and radioactivity is measured throughout the experiment, typically for about one hour. Although the technique is temporally and spatially less precise than BOLD-fMRI, it has the advantage of biological specificity yielding estimates of glucose metabolism in the brain that is independent of blood flow (*111*). Moreover, it can be combined with simultaneous BOLD-fMRI for informing about the metabolic bases of the haemodynamic signal. For example, although task-positive activations during working memory task align well across fPET and BOLD fMRI, the common default mode network "deactivations" observed in BOLD signal are completely absent glucose metabolism indicating the putative role of energy-demanding suppression of task-irrelevant activity (*111*). Although this approach has been applied for mapping e.g., sensory, motor, and cognitive functions (*111, 112*), its potential in affective imaging remains to be seen.

4.2. Total-body PET imaging

Emotions are allostatic processes that transfer the relationship between the environment and the desired bodily states into behaviour that supports homeostasis and well-being (*113*). Subjectively experienced emotions (e.g. "I'm anxious") include a central representation of the body's physiological state (*114, 115*), and bodily symptoms such as chest and stomach pain and sweating and trembling are central in affective disorders such as anxiety. Negative emotions are established risk factors for somatic illnesses such as cardiovascular diseases (CVDs) (*116*) and conversely, CVDs are associated with heightened anxiety (*117*) highlighting the link between negative emotions, bodily functions, and somatic health. The systems-level interaction between brain and periphery in emotions and their dysfunctions have remained poorly understood and the role of the autonomic nervous system in emotions has been hotly debated through the history of psychology (*113, 118, 119*). The debate is focused on how specific peripheral autonomic changes engage emotion circuits in the brain, and how changes in the central emotional state lead to functional changes in the peripheral organs (*120*). As central and peripheral emotional symptoms are at the core of psychiatric disorders, mapping the crosstalk of emotion circuits spanning the brain and body in health and disease has also gained significant momentum. This has however been difficult to actualise due to lacking technology. Although modern neuroimaging methods allow mapping brain basis of emotion and cognition, they do not allow simultaneous measurement of the high-dimensional physiological state of the brain and peripheral organs (*121*). The major advantage of PET is that the acquisition of the projection data is not limited by physical (e.g. gantry rotation in CT) or electronic (e.g. pulse sequences in MRI) scanning. Instead, the limits arise from the counting statistics of coincident photon detection. Conventional PET scanners have poor sensitivity (<1%) for whole-body PET scans for two reasons (*4*). First, roughly 85%–90% of the body always is outside the FOV of the scanner thus yielding no signal. Second, even for tissues and organs within the FOV, only less than 5% of the gamma rays can be collected, as the radiation is emitted isotopically, and it does not intercept the detector rings (*122*).

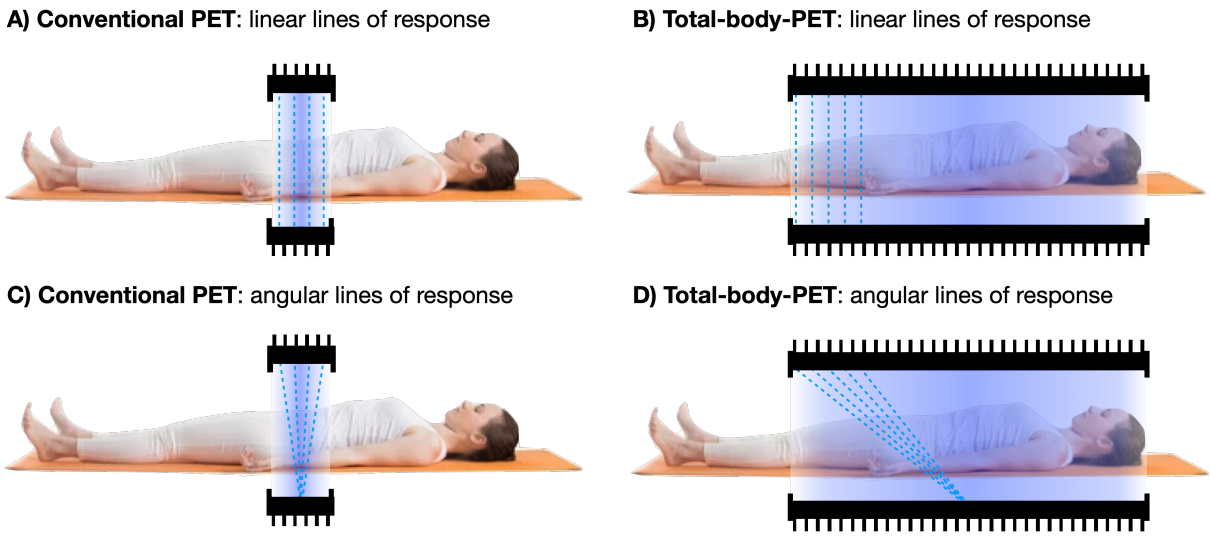

Figure 4. Illustration of the increased number of gamma counts in total-body PET.
The final frontier – principles for conducting simultaneous whole-body studies allowing systems-level biological imaging across organs.

Total-body PET resolves both these problems by extending the detector rings so that they cover practically the whole body (**Figure 4**). The axial field of view of the commercially available Siemens Quadra total-body PET is 106 cm which is four times longer than the axial field of view in conventional PET/CT scanners. It covers the whole-body from head to approximately mid-thigh in a single scan in most subjects/patients leading to 24-fold increase in gamma counts in head to-thigh scan. This allows, for the first time, dynamic imaging of the brain and all internal organs. The SNR in a reconstructed PET scan is $\sqrt{N}$, where N is the number of detected events. The number of detected events depend on scanner sensitivity (S), injected activity (A) and imaging time (T) scaled by constant k. Thus, $SNR = k\sqrt{S \cdot A \cdot T}$. This sensitivity gain from total-body-PET can be used for Increasing SNR by a factor of $\sqrt{24}$=4.9, reducing imaging times or injected activity with a factor of 24 (allowing more injections per study), or using temporal information in the signal for tissue-specific modelling.

Since the advent of functional magnetic resonance imaging (*17*) quantitative perfusion-based PET studies of human brain activity fell out of favour due to the complexity, low temporal precision and associated radiation load. With the advent of total-body PET the quantitative dynamic PET imaging of the brain is again at the prime because it can be combined with simultaneous imaging of the peripheral organs (*123*) and because the modern total-body PET scanners yield ultrasensitive sub-second temporal precision (*4, 124*). When CBF is measured with diffusible tracers in PET, it allows measuring blood flow at the nutrient capillary level. Thus, parameters derived within short (1-s) time windows likely show excellent correlation with postsynaptic activity with little hemodynamic lag. Accordingly, the total-body PET method allows, for the first time, true biological quantification of the brain-body loops in human emotion circuits (**Figure 5**). The total-body PET approach (*4, 124*) allows simultaneously measuring the physiology of the emotion circuits across the brain and peripheral organs and mapping their functioning in health and disease. This shifts the focus from dualistic studies on brain or periphery to high-resolution imaging across the whole body, creating an innovative multisystem biology approach for studying emotions and their dysfunctions.

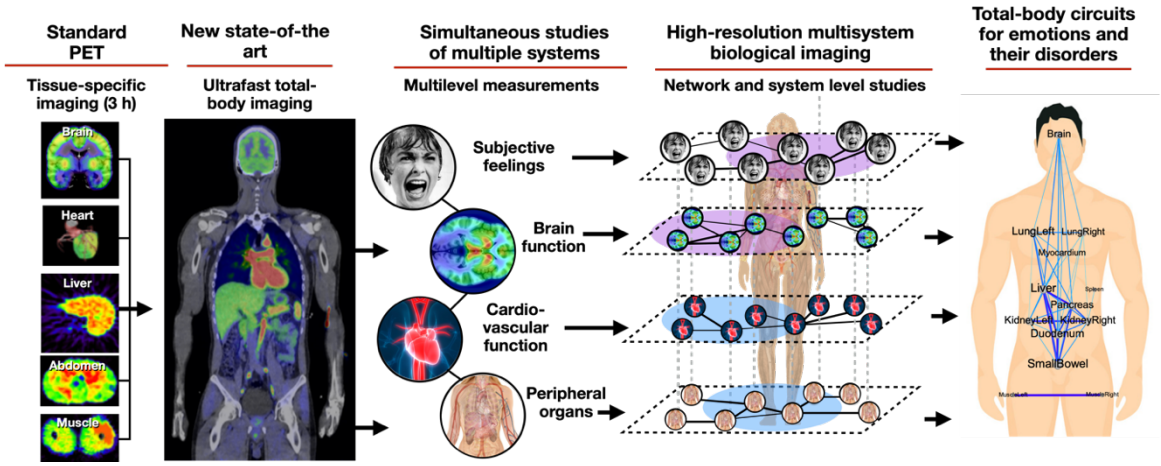

Figure 5. Illustration of total-body PET in systems-level emotion science

4.3. Novel targets

In addition to traditional neurochemical targets, PET imaging can now reach "beyond the receptor" downstream into the signaling cascade, where multiple neurochemical inputs are being integrated. Phosphodiesterases (PDE), which exist in multiple isoforms, are enzymes that mediate the effects of various neurotransmitters. PET studies have shown PDE10A isoform abnormalities in schizophrenia (*98*) and PDE4 isoform reduction in major depression (*125*). Future studies must unravel the relationships between neurochemical signaling (*e.g.*, dopamine, glutamate, opioid) and PDE activity in brain function. Synaptic density can now be imaged in the living human brain. Synaptic vesicle protein 2A (SV2A) is a glycoprotein that is expressed at the membranes of brain synaptic vesicles. SV2A can be imaged with PET using novel radioligands, such as [^{11}C]UCB-J (*126*). In neuropsychiatric brain imaging, alterations in SV2A expression have been documented so far in schizophrenia (*127*), major depression (*128*), cocaine use disorder (*129*), and cannabis use disorder (*130*). Interestingly, lower synaptic density has also been reported in obesity (*131*) . SV2A PET imaging is an important new tool in the arsenal of multimodal brain imaging in neuropsychiatric disorders. Finally, epigenetic regulation of gene expression is modulated by histone acetylation, which is, in turn, controlled by histone deacetylases (HDAC). HDAC can be targeted using PET and selective radioligands (*132*). So far, altered HDAC expression has been shown in bipolar depression (*133*), schizophrenia (*134*), and Alzheimers's disease (*135*). Imaging the epigenetic regulation in the human brain is expected to yield important information about the pathogenesis of neuropsychiatric disorders and will help disentangle the complex interplay between genetic and environmental factors.

5. Conclusions

In 2014 the journal NeuroImage published a controversial commentary "PET neuroimaging: the white elephant packs his trunk?", suggesting that PET neuroscience would soon be past its best before date (*136*). As commentaries to this paper quickly suggested (*137, 138*), the PET community was far from dwindling – quite the contrary, it has been continuously expanding and pushing the boundaries of molecule-level tomography in living humans with many molecule targets that could not be covered in this brief introduction. As elaborated on above, recent developments have enabled direct mapping of synaptic density (*139*) and epigenetic dysfunction imaging via histone deacetylase targets (*140*). Functional metabolic imaging, simultaneous PET-fMRI studies, and most recently, total-body PET imaging (*4, 124*) will pave the way for multilevel understanding of the human brain and its affective circuits spanning the whole body.

Acknowledgements
This work was supported by the Academy of Finland (#332225), Sigrid Juselius Stiftelse, and Signe och Ane Gylllengerg's Stiftelse. We thank Jouni Tuisku for and Mueez U-Din for their help with preparing the figures.

References

1. W. Wadsak, M. Mitterhauser, Basics and principles of radiopharmaceuticals for PET/CT. *European journal of radiology* **73**, 461-469 (2010).
2. S. Surti, Update on time-of-flight PET imaging. *Journal of nuclear medicine : official publication, Society of Nuclear Medicine* **56**, 98-105 (2015).
3. W. W. Moses, Fundamental limits of spatial resolution in PET. *Nuclear Instruments and Methods in Physics Research Section A: Accelerators, Spectrometers, Detectors and Associated Equipment* **648**, S236-S240 (2011).
4. X. Zhang *et al.*, Subsecond total-body imaging using ultrasensitive positron emission tomography. *Proceedings of the National Academy of Sciences* **117**, 2265 (2020).
5. A. T. Joseph, Understanding the Standardized Uptake Value, Its Methods, and Implications for Usage. *J. Nucl. Med.* **45**, 1431 (2004).
6. R. N. Gunn, A. A. Lammertsma, S. P. Hume, V. J. Cunningham, Parametric imaging of ligand-receptor binding in PET using a simplified reference region model. *Neuroimage* **6**, 279-287 (1997).
7. A. A. Lammertsma, S. P. Hume, Simplified reference tissue model for PET receptor studies. *Neuroimage* **4**, 153-158 (1996).
8. A. L. Smith *et al.*, Initial investigation of three selective and potent small molecule oxytocin receptor PET ligands in New World monkeys. *Bioorganic & Medicinal Chemistry Letters* **26**, 3370-3375 (2016).
9. T. Kantonen *et al.*, Obesity risk is associated with altered cerebral glucose metabolism and decreased mu-opioid and CB1-receptor availability *International Journal of Obesity.*, (2021).
10. L. Tuominen *et al.*, Temperament trait Harm Avoidance associates with mu-opioid receptor availability in frontal cortex: A PET study using C-11 carfentanil. *Neuroimage* **61**, 670-676 (2012).
11. H. K. Karlsson *et al.*, Weight loss after bariatric surgery normalizes brain opioid receptors in morbid obesity. *Molecular psychiatry* **21**, 1057-1062 (2016).
12. J. H. Meyer *et al.*, Serotonin Transporter Occupancy of Five Selective Serotonin Reuptake Inhibitors at Different Doses: An [11C]DASB Positron Emission Tomography Study. *Am. J. Psychiat.* **161**, 826-835 (2004).
13. J. K. Zubieta *et al.*, Regional mu opioid receptor regulation of sensory and affective dimensions of pain. *Science* **293**, 311-315 (2001).
14. E. M. Reiman *et al.*, Neuroanatomical correlates of externally and internally generated human emotion. *The American journal of psychiatry* **154**, 918-925 (1997).
15. S. Kajander *et al.*, Cardiac Positron Emission Tomography/Computed Tomography Imaging Accurately Detects Anatomically and Functionally Significant Coronary Artery Disease. *Circulation* **122**, 603-613 (2010).
16. A. R. Damasio *et al.*, Subcortical and cortical brain activity during the feeling of self-generated emotions. *Nature neuroscience* **3**, 1049-1056 (2000).
17. S. Ogawa, T. M. Lee, A. R. Kay, D. W. Tank, Brain magnetic resonance imaging with contrast dependent on blood oxygenation. *Proc. Natl. Acad. Sci. U. S. A.* **87**, 9868-9872 (1990).
18. M. D'Esposito, E. Zarahn, G. K. Aguirre, Event-related functional MRI: implications for cognitive psychology. *Psychol Bull* **125**, 155-164 (1999).
19. L. Sokoloff, Energetics of functional activation in neural tissues. *Neurochemical research* **24**, 321-329 (1999).

20. M. E. Raichle, Two views of brain function. *Trends Cogn. Sci.* **14**, 180-190 (2010).
21. L. Laaksonen *et al.*, Comparative effects of dexmedetomidine, propofol, sevoflurane, and S-ketamine on regional cerebral glucose metabolism in humans: a positron emission tomography study. *Br J Anaesth* **121**, 281-290 (2018).
22. J. P. Taglialatela, J. L. Russell, J. A. Schaeffer, W. D. Hopkins, Communicative Signaling Activates Broca's Homolog in Chimpanzees. *Curr. Biol.* **18**, 343-348 (2008).
23. L. Su *et al.*, Cerebral metabolism in major depressive disorder: a voxel-based meta-analysis of positron emission tomography studies. *BMC Psychiatry* **14**, 321 (2014).
24. K. Pak *et al.*, Brain glucose metabolism and ageing: A 5-year longitudinal study in a large PET cohort. *Diabetes Care*, (2022).
25. A. Raine, J. Stoddard, S. Bihrle, M. Buchsbaum, Prefrontal glucose deficits in murderers lacking psychosocial deprivation. *Neuropsychiatr. Neuropsychol. Behav. Neurol.* **11**, 1-7 (1998).
26. D. H. Zald, The human amygdala and the emotional evaluation of sensory stimuli. *Brain research. Brain research reviews* **41**, 88-123 (2003).
27. A. J. Shackman *et al.*, Neural mechanisms underlying heterogeneity in the presentation of anxious temperament. *Proceedings of the National Academy of Sciences* **110**, 6145-6150 (2013).
28. S. Marek *et al.*, Reproducible brain-wide association studies require thousands of individuals. *Nature* **603**, 654-660 (2022).
29. E. Rebelos *et al.*, Insulin Resistance Is Associated With Enhanced Brain Glucose Uptake During Euglycemic Hyperinsulinemia: A Large-Scale PET Cohort. *Diabetes Care* **44**, 788 (2021).
30. J. K. Rowlett, D. M. Platt, S. Lelas, J. R. Atack, G. R. Dawson, Different GABAA receptor subtypes mediate the anxiolytic, abuse-related, and motor effects of benzodiazepine-like drugs in primates. *Proceedings of the National Academy of Sciences* **102**, 915-920 (2005).
31. J. D. Andersson, D. Matuskey, S. J. Finnema, Positron emission tomography imaging of the γ-aminobutyric acid system. *Neurosci Lett* **691**, 35-43 (2019).
32. V. J. Majo, J. Prabhakaran, J. J. Mann, J. S. D. Kumar, PET and SPECT tracers for glutamate receptors. *Drug Discovery Today* **18**, 173-184 (2013).
33. S. Manninen *et al.*, Social laughter triggers endogenous opioid release in humans. *The Journal of Neuroscience* **37**, 6125-6131 (2017).
34. L. Nummenmaa *et al.*, Lowered endogenous mu-opioid receptor availability in subclinical depression and anxiety. *Neuropsychopharmacology*, (2020).
35. L. Farde, H. Hall, E. Ehrin, G. Sedvall, Quantitative analysis of D2 dopamine receptor binding in the living human brain by PET. *Science* **231**, 258-261 (1986).
36. D. F. Wong *et al.*, Positron emission tomography reveals elevated D2 dopamine receptors in drug-naive schizophrenics. *Science* **234**, 1558-1563 (1986).
37. L. Farde *et al.*, No D2 receptor increase in PET study of schizophrenia. *Arch Gen Psychiatry* **44**, 671-672 (1987).
38. A. Abi-Dargham *et al.*, Increased striatal dopamine transmission in schizophrenia: confirmation in a second cohort. *The American journal of psychiatry* **155**, 761-767 (1998).
39. P. Cumming, A. Abi-Dargham, G. Gründer, Molecular imaging of schizophrenia: Neurochemical findings in a heterogeneous and evolving disorder. *Behavioural brain research* **398**, 113004 (2021).
40. N. D. Volkow, J. S. Fowler, G. J. Wang, R. Baler, F. Telang, Imaging dopamine's role in drug abuse and addiction. *Neuropharmacology* **56**, 3-8 (2009).
41. N. D. Volkow *et al.*, Decreases in dopamine receptors but not in dopamine transporters in alcoholics. *Alcoholism, clinical and experimental research* **20**, 1594-1598 (1996).
42. N. D. Volkow *et al.*, Low level of brain dopamine D2 receptors in methamphetamine abusers: association with metabolism in the orbitofrontal cortex. *The American journal of psychiatry* **158**, 2015-2021 (2001).

43. D. Martinez *et al.*, Deficits in dopamine D(2) receptors and presynaptic dopamine in heroin dependence: commonalities and differences with other types of addiction. *Biological psychiatry* **71**, 192-198 (2012).
44. J. Joutsa *et al.*, Mesolimbic dopamine release is linked to symptom severity in pathological gambling. *Neuroimage* **60**, 1992-1999 (2012).
45. P. M. Johnson, P. J. Kenny, Dopamine D2 receptors in addiction-like reward dysfunction and compulsive eating in obese rats. *Nature neuroscience* **13**, 635-641 (2010).
46. G. J. Wang *et al.*, Brain dopamine and obesity. *Lancet* **357**, 354-357 (2001).
47. B. A. de Weijer *et al.*, Lower striatal dopamine D2/3 receptor availability in obese compared with non-obese subjects. *EJNMMI research* **1**, 37 (2011).
48. N. D. Volkow *et al.*, Low dopamine striatal D2 receptors are associated with prefrontal metabolism in obese subjects: possible contributing factors. *Neuroimage* **42**, 1537-1543 (2008).
49. K. E. Steele *et al.*, Alterations of central dopamine receptors before and after gastric bypass surgery. *Obesity surgery* **20**, 369-374 (2010).
50. L. T. Haltia *et al.*, Effects of intravenous glucose on dopaminergic function in the human brain in vivo. *Synapse (New York, N.Y.)* **61**, 748-756 (2007).
51. L. T. Haltia *et al.*, Effects of intravenous placebo with glucose expectation on human basal ganglia dopaminergic function. *Synapse (New York, N.Y.)* **62**, 682-688 (2008).
52. D. M. Small, M. Jones-Gotman, A. Dagher, Feeding-induced dopamine release in dorsal striatum correlates with meal pleasantness ratings in healthy human volunteers. *Neuroimage* **19**, 1709-1715 (2003).
53. V. N. Salimpoor, M. Benovoy, K. Larcher, A. Dagher, R. J. Zatorre, Anatomically distinct dopamine release during anticipation and experience of peak emotion to music. *Nature neuroscience* **14**, 257-U355 (2011).
54. M. J. Koepp *et al.*, Evidence for striatal dopamine release during a video game. *Nature* **393**, 266-268 (1998).
55. L. S. Jonasson *et al.*, Dopamine release in nucleus accumbens during rewarded task switching measured by C-11 raclopride. *Neuroimage* **99**, 357-364 (2014).
56. R. D. Badgaiyan, A. J. Fischman, N. M. Alpert, Dopamine release during human emotional processing. *Neuroimage* **47**, 2041-2045 (2009).
57. R. D. Badgaiyan, Dopamine is released in the striatum during human emotional processing. *Neuroreport* **21**, 1172-1176 (2010).
58. G. Henriksen, F. Willoch, Imaging of opioid receptors in the central nervous system. *Brain* **131**, 1171-1196 (2008).
59. L. Nummenmaa, L. J. Tuominen, Opioid system and human emotions. *Br. J. Pharmacol.* **175**, 2737-2749 (2018).
60. T. Kantonen *et al.*, Interindividual variability and lateralization of μ-opioid receptors in the human brain. *Neuroimage*, (2020).
61. A. Heinz *et al.*, Correlation of stable elevations in striatal mu-opioid receptor availability in detoxified alcoholic patients with alcohol craving: a positron emission tomography study using carbon 11-labeled carfentanil. *Arch Gen Psychiatry* **62**, 57-64 (2005).
62. E. M. Weerts *et al.*, Positron emission tomography imaging of mu- and delta-opioid receptor binding in alcohol-dependent and healthy control subjects. *Alcoholism, clinical and experimental research* **35**, 2162-2173 (2011).
63. D. A. Gorelick *et al.*, Imaging brain mu-opioid receptors in abstinent cocaine users: time course and relation to cocaine craving. *Biological psychiatry* **57**, 1573-1582 (2005).
64. T. Koch, V. Hollt, Role of receptor internalization in opioid tolerance and dependence. *Pharmacology & therapeutics* **117**, 199-206 (2008).

65. J. L. Whistler, Examining the role of mu opioid receptor endocytosis in the beneficial and side-effects of prolonged opioid use: from a symposium on new concepts in mu-opioid pharmacology. *Drug and alcohol dependence* **121**, 189-204 (2012).
66. H. K. Karlsson *et al.*, Obesity Is Associated with Decreased mu-Opioid But Unaltered Dopamine D-2 Receptor Availability in the Brain. *J. Neurosci.* **35**, 3959-3965 (2015).
67. L. Tuominen *et al.*, Aberrant mesolimbic dopamine-opiate interaction in obesity. *Neuroimage* **122**, 80-86 (2015).
68. P. R. Burghardt, A. E. Rothberg, K. E. Dykhuis, C. F. Burant, J. K. Zubieta, Endogenous Opioid Mechanisms Are Implicated in Obesity and Weight Loss in Humans. *J. Clin. Endocrinol. Metab.* **100**, 3193-3201 (2015).
69. J. Majuri *et al.*, Dopamine and Opioid Neurotransmission in Behavioral Addictions: A Comparative PET Study in Pathological Gambling and Binge Eating. *Neuropsychopharmacology*, 1169-1177 (2016).
70. B. Bencherif *et al.*, Pain activation of human supraspinal opioid pathways as demonstrated by C-11 -carfentanil and positron emission tomography (PET). *Pain* **99**, 589-598 (2002).
71. D. J. Scott, C. S. Stohler, R. A. Koeppe, J. K. Zubieta, Time-course of change in C-11 carfentanil and C-11 raclopride binding potential after a nonpharmacological challenge. *Synapse (New York, N.Y.)* **61**, 707-714 (2007).
72. J. J. Tuulari *et al.*, Feeding Releases Endogenous Opioids in Humans. *J. Neurosci.* **37**, 8284-8291 (2017).
73. P. Jern *et al.*, Endogenous opioid release following orgasm in man: A combined PET-fMRI study. *J. Nucl. Med.*, (2023).
74. H. Boecker *et al.*, The Runner's High: Opioidergic Mechanisms in the Human Brain. *Cereb. Cortex* **18**, 2523-2531 (2008).
75. T. Saanijoki *et al.*, Opioid Release after High-Intensity Interval Training in Healthy Human Subjects. *Neuropsychopharmacology*, (2017).
76. M. J. Koepp *et al.*, Evidence for endogenous opioid release in the amygdala during positive emotion. *Neuroimage* **44**, 252-256 (2009).
77. S. E. Kennedy, R. A. Koeppe, E. A. Young, J. K. Zubieta, Dysregulation of endogenous opioid emotion regulation circuitry in major depression in women. *Arch. Gen. Psychiatry* **63**, 1199-1208 (2006).
78. D. T. Hsu *et al.*, It still hurts: altered endogenous opioid activity in the brain during social rejection and acceptance in major depressive disorder. *Molecular psychiatry* **20**, 193-200 (2015).
79. W. C. Drevets *et al.*, Pet imaging of serotonin 1A receptor binding in depression. *Biological psychiatry* **46**, 1375-1387 (1999).
80. G. Gryglewski, R. Lanzenberger, G. S. Kranz, P. Cumming, Meta-analysis of molecular imaging of serotonin transporters in major depression. *J. Cereb. Blood Flow Metab.* **34**, 1096-1103 (2014).
81. N. Risch *et al.*, Interaction Between the Serotonin Transporter Gene (5-HTTLPR), Stressful Life Events, and Risk of Depression A Meta-analysis. *JAMA-J. Am. Med. Assoc.* **301**, 2462-2471 (2009).
82. R. V. Parsey *et al.*, Higher serotonin 1A binding in a second major depression cohort: modeling and reference region considerations. *Biological psychiatry* **68**, 170-178 (2010).
83. J. Hirvonen *et al.*, Decreased brain serotonin 5-HT1A receptor availability in medication-naive patients with major depressive disorder: an in-vivo imaging study using PET and [carbonyl-11C]WAY-100635. *Int J Neuropsychopharmacol* **11**, 465-476 (2008).
84. S. Shrestha *et al.*, Serotonin-1A receptors in major depression quantified using PET: controversies, confounds, and recommendations. *Neuroimage* **59**, 3243-3251 (2012).

85. M. J. Lan *et al.*, Serotonin 1A Receptor Binding of [11C]CUMI-101 in Bipolar Depression Quantified Using Positron Emission Tomography: Relationship to Psychopathology and Antidepressant Response. *Int J Neuropsychopharmacol* **25**, 534-544 (2022).
86. K. Köhler-Forsberg *et al.*, Serotonin 4 Receptor Brain Binding in Major Depressive Disorder and Association With Memory Dysfunction. *JAMA Psychiatry* **80**, 296-304 (2023).
87. M. Tiger *et al.*, Low serotonin1B receptor binding potential in the anterior cingulate cortex in drug-free patients with recurrent major depressive disorder. *Psychiatry Res Neuroimaging* **253**, 36-42 (2016).
88. D. Erritzoe *et al.*, Brain Serotonin Release Is Reduced in Patients With Depression: A [(11)C]Cimbi-36 Positron Emission Tomography Study With a d-Amphetamine Challenge. *Biological psychiatry* **93**, 1089-1098 (2023).
89. R. Mechoulam, L. A. Parker, The endocannabinoid system and the brain. *Annu Rev Psychol* **64**, 21-47 (2013).
90. T. C. Kirkham, C. M. Williams, F. Fezza, V. Di Marzo, Endocannabinoid levels in rat limbic forebrain and hypothalamus in relation to fasting, feeding and satiation: stimulation of eating by 2-arachidonoyl glycerol. *Br J Pharmacol* **136**, 550-557 (2002).
91. G. E. Terry *et al.*, Quantitation of cannabinoid CB1 receptors in healthy human brain using positron emission tomography and an inverse agonist radioligand. *Neuroimage* **48**, 362-370 (2009).
92. G. E. Terry *et al.*, Imaging and quantitation of cannabinoid CB1 receptors in human and monkey brains using (18)F-labeled inverse agonist radioligands. *Journal of nuclear medicine : official publication, Society of Nuclear Medicine* **51**, 112-120 (2010).
93. D. F. Wong *et al.*, Quantification of cerebral cannabinoid receptors subtype 1 (CB1) in healthy subjects and schizophrenia by the novel PET radioligand [11C]OMAR. *Neuroimage* **52**, 1505-1513 (2010).
94. H. D. Burns *et al.*, [18F]MK-9470, a positron emission tomography (PET) tracer for in vivo human PET brain imaging of the cannabinoid-1 receptor. *Proc Natl Acad Sci U S A* **104**, 9800-9805 (2007).
95. J. Hirvonen, In vivo imaging of the cannabinoid CB1 receptor with positron emission tomography. *Clin Pharmacol Ther* **97**, 565-567 (2015).
96. J. Hirvonen *et al.*, Reversible and regionally selective downregulation of brain cannabinoid CB1 receptors in chronic daily cannabis smokers. *Molecular psychiatry* **17**, 642-649 (2012).
97. J. Hirvonen *et al.*, Reduced cannabinoid CB1 receptor binding in alcohol dependence measured with positron emission tomography. *Molecular psychiatry* **18**, 916-921 (2013).
98. J. Hirvonen *et al.*, Decreased Cannabinoid CB(1) Receptors in Male Tobacco Smokers Examined With Positron Emission Tomography. *Biological psychiatry* **84**, 715-721 (2018).
99. T. Kantonen *et al.*, Cerebral μ-opioid and CB1 receptor systems have distinct roles in human feeding behavior. *Translational Psychiatry* **11**, 442 (2021).
100. J. Hirvonen *et al.*, Effects of Insulin on Brain Glucose Metabolism in Impaired Glucose Tolerance. *Diabetes* **60**, 443-447 (2011).
101. L. Nummenmaa *et al.*, Dorsal Striatum and Its Limbic Connectivity Mediate Abnormal Anticipatory Reward Processing in Obesity. *PLoS One* **7**, 10 (2012).
102. T. Karjalainen *et al.*, Opioidergic Regulation of Emotional Arousal: A Combined PET-fMRI Study. *Cerebral cortex (New York, N.Y. : 1991)*, (2018).
103. T. Karjalainen *et al.*, Dissociable Roles of Cerebral mu-Opioid and Type 2 Dopamine Receptors in Vicarious Pain: A Combined PET-fMRI Study. *Cerebral cortex (New York, N.Y. : 1991)*, 1-10 (2017).
104. P. M. Fisher *et al.*, Medial Prefrontal Cortex 5-HT2A Density Is Correlated with Amygdala Reactivity, Response Habituation, and Functional Coupling. *Cereb. Cortex* **19**, 2499-2507 (2009).

105. P. M. Fisher *et al.*, Capacity for 5-HT 1A –mediated autoregulation predicts amygdala reactivity. *Nature neuroscience* **9**, 1362 (2006).
106. S. Selvaraj *et al.*, Presynaptic Serotoninergic Regulation of Emotional Processing: A Multimodal Brain Imaging Study. *Biological psychiatry* **78**, 563-571 (2015).
107. R. A. Rhodes *et al.*, Human 5-HT Transporter Availability Predicts Amygdala Reactivity In Vivo. *J. Neurosci.* **27**, 9233-9237 (2007).
108. N. K. Logothetis, B. A. Wandell, Interpreting the BOLD signal. *Annu. Rev. Physiol.* **66**, 735-769 (2004).
109. E. M. C. Hillman, Coupling Mechanism and Significance of the BOLD Signal: A Status Report. *Annual Review of Neuroscience* **37**, 161-181 (2014).
110. M. Villien *et al.*, Dynamic functional imaging of brain glucose utilization using fPET-FDG. *Neuroimage* **100**, 192-199 (2014).
111. L. J. Stiernman *et al.*, Dissociations between glucose metabolism and blood oxygenation in the human default mode network revealed by simultaneous PET-fMRI. *Proceedings of the National Academy of Sciences* **118**, e2021913118 (2021).
112. A. Hahn *et al.*, Quantification of Task-Specific Glucose Metabolism with Constant Infusion of 18F-FDG. *Journal of nuclear medicine : official publication, Society of Nuclear Medicine* **57**, 1933-1940 (2016).
113. L. Nummenmaa, E. Glerean, R. Hari, J. K. Hietanen, Bodily maps of emotions. *Proc. Natl. Acad. Sci. U. S. A.* **111**, 646-651 (2014).
114. A. Damasio, G. B. Carvalho, The nature of feelings: evolutionary and neurobiological origins. *Nature Reviews Neuroscience* **14**, 143-152 (2013).
115. L. Nummenmaa, R. Hari, J. K. Hietanen, E. Glerean, Maps of subjective feelings. *Proc. Natl. Acad. Sci. U. S. A.* **115**, 9198–9203 (2018).
116. D. J. Brotman, S. H. Golden, I. S. Wittstein, The cardiovascular toll of stress. *The Lancet* **370**, 1089-1100 (2007).
117. T. A. Hanssen, J. E. Nordrehaug, G. E. Eide, I. Bjelland, B. Rokne, Anxiety and depression after acute myocardial infarction: an 18-month follow-up study with repeated measures and comparison with a reference population. *Eur J Cardiovasc Prev Rehabil* **16**, 651-659 (2009).
118. W. James, What is an emotion? *Mind* **9**, 188-205 (1884).
119. E. H. Siegel *et al.*, Emotion fingerprints or emotion populations? A meta-analytic investigation of autonomic features of emotion categories. *Psychol. Bull.* **144**, 343-393 (2018).
120. L. Nummenmaa, H. Saarimäki, Emotions as discrete patterns of systemic activity. *Neuroscience Letters*, (2017).
121. Hugo D. Critchley, Neil A. Harrison, Visceral Influences on Brain and Behavior. *Neuron* **77**, 624-638 (2013).
122. S. R. Cherry *et al.*, Total-Body PET: Maximizing Sensitivity to Create New Opportunities for Clinical Research and Patient Care. *Journal of nuclear medicine : official publication, Society of Nuclear Medicine* **59**, 3-12 (2018).
123. H. Tan *et al.*, Total-Body PET/CT: Current Applications and Future Perspectives. *American Journal of Roentgenology* **215**, 325-337 (2020).
124. S. R. Cherry *et al.*, Total-body imaging: Transforming the role of positron emission tomography. *Sci. Transl. Med.* **9**, eaaf6169 (2017).
125. M. Fujita *et al.*, Downregulation of brain phosphodiesterase type IV measured with 11C-(R)-rolipram positron emission tomography in major depressive disorder. *Biological psychiatry* **72**, 548-554 (2012).
126. S. J. Finnema *et al.*, Kinetic evaluation and test-retest reproducibility of [(11)C]UCB-J, a novel radioligand for positron emission tomography imaging of synaptic vesicle glycoprotein 2A in humans. *J Cereb Blood Flow Metab* **38**, 2041-2052 (2018).

127. E. C. Onwordi *et al.*, Synaptic density marker SV2A is reduced in schizophrenia patients and unaffected by antipsychotics in rats. *Nat Commun* **11**, 246 (2020).
128. S. E. Holmes *et al.*, Lower synaptic density is associated with depression severity and network alterations. *Nat Commun* **10**, 1529 (2019).
129. G. A. Angarita *et al.*, Lower prefrontal cortical synaptic vesicle binding in cocaine use disorder: An exploratory (11) C-UCB-J positron emission tomography study in humans. *Addict Biol* **27**, e13123 (2022).
130. D. C. D'Souza *et al.*, Preliminary in vivo evidence of lower hippocampal synaptic density in cannabis use disorder. *Molecular psychiatry* **26**, 3192-3200 (2021).
131. R. H. Asch *et al.*, Lower synaptic density is associated with psychiatric and cognitive alterations in obesity. *Neuropsychopharmacology* **47**, 543-552 (2022).
132. H. Y. Wey *et al.*, Insights into neuroepigenetics through human histone deacetylase PET imaging. *Sci Transl Med* **8**, 351ra106 (2016).
133. C. J. Tseng *et al.*, In vivo human brain expression of histone deacetylases in bipolar disorder. *Transl Psychiatry* **10**, 224 (2020).
134. T. M. Gilbert *et al.*, PET neuroimaging reveals histone deacetylase dysregulation in schizophrenia. *J Clin Invest* **129**, 364-372 (2019).
135. T. A. Pascoal *et al.*, [(11)C]Martinostat PET analysis reveals reduced HDAC I availability in Alzheimer's disease. *Nat Commun* **13**, 4171 (2022).
136. P. Cumming, PET Neuroimaging: The White Elephant Packs His Trunk? *Neuroimage* **84**, 1094-1100 (2014).
137. B. Horwitz, K. Simonyan, PET neuroimaging: Plenty of studies still need to be performed: Comment on Cumming: "PET Neuroimaging: The White Elephant Packs His Trunk?". *Neuroimage* **84**, 1101-1103 (2014).
138. R. N. Gunn, E. A. Rabiner, PET neuroimaging: The elephant unpacks his trunk: Comment on Cumming: "PET neuroimaging: The white elephant packs his trunk?". *Neuroimage* **94**, 408-410 (2014).
139. S. J. Finnema *et al.*, Imaging synaptic density in the living human brain. *Sci. Transl. Med.* **8**, 9 (2016).
140. H.-Y. Wey *et al.*, Insights into neuroepigenetics through human histone deacetylase PET imaging. *Sci. Transl. Med.* **8**, 351ra106-351ra106 (2016).